frontiers | Frontiers in Materials

TYPE Original Research
PUBLISHED 21 May 2025
DOI 10.3389/fmats.2025.1585978

OPEN ACCESS

EDITED BY
Augusto Cannone Falchetto,
University of Padua, Italy

REVIEWED BY
Iurii Vozniak,
Polish Academy of Sciences, Poland
Yuxuan Sun,
Aalto University, Finland

*CORRESPONDENCE
Peng Wang,
wang.peng@rioh.cn
Pengfei Li,
1208384125@qq.com

RECEIVED 01 March 2025
ACCEPTED 05 May 2025
PUBLISHED 21 May 2025

CITATION
He Y, Li H, He C, Zhang Y, Wang P and Li P (2025) Effect of foaming water dosage on mechanical properties of warm foamed asphalt mixture.
Front. Mater. 12:1585978.
doi: 10.3389/fmats.2025.1585978

Effect of foaming water dosage on mechanical properties of warm foamed asphalt mixture

Yan He[1], Haibo Li[1], Chuanping He[1], Yangpeng Zhang[2], Peng Wang[3]* and Pengfei Li[3]*

[1]Guangxi Xinfazhan Communication Group Co., LTD, Nanning, China, [2]Guangxi Transportation Science and Technology Co., LTD., Nanning, China, [3]Research Institute of Highway Ministry of Transport, Beijing, China

This study investigated the impact of foaming water consumption on the mechanical properties of foam warm mix matrix asphalt mixture (FWMAM) and foam warm mix SBS-modified asphalt mixture (FWMAM-SBS) through comparative analysis with conventional hot mix matrix asphalt mixture (HMAM) and hot mix SBS-modified asphalt mixture (HMAM-SBS). The results showed that: The tensile strength ratio (TSR) of FWMAM showed no significant difference from HMAM, whereas HMAM-SBS exhibited slightly reduced TSR compared to FWMAM-SBS. The rutting resistance of FWMAM was superior to HMAM and enhanced progressively as the water consumption increased, while the anti-rutting performance of FWMAM-SBS was less affected by the foaming water consumption. The low-temperature cracking resistance of FWMAM was generally weaker than that of HMAM, while the opposite is true for FWMAM-SBS, with lower temperatures amplifying the influence of foaming water content. The master curve distribution characteristics of the FWMAM are consistent with those of the HMAM, and the water consumption is positively correlated with the modulus of the FWMAM and has a lower effect on the FWMAM-SBS at the conventional loading frequency. For fatigue life, both FWMAM and FWMAM-SBS outperform the corresponding hot-mix mixture. The fatigue life of FWMAM gradually decreased with increasing foaming water content, while FWMAM-SBS initially increased and then decreased, peaking at 2% water content, while fatigue life of FWMAM at low strain level conditions is roughly 1.2 times higher than that of the HMAM. Based on mechanical performance and foaming efficacy, optimal water consumption thresholds are proposed: ≤1% for matrix asphalt and ≤2% for SBS-modified asphalt.

KEYWORDS

road engineering, foam warm mix asphalt mixture, foaming water dosage, moisture damage resistance, fatigue resistance

1 Introduction

As the process of global industrialisation continues to accelerate, environmental protection has become a crucial issue in the development of today's society. In the field of road engineering, the traditional asphalt mixture technology consumes a lot of energy during production and construction, and releases large amounts of asphalt fumes, dust and harmful gases such as CO, SO (Woszuk and Franus, 2017; Yu et al., 2018). These not only cause serious air pollution and endanger the health of neighbouring residents, but are also

inconsistent with the concept of sustainable development (Huang et al., 2022). Therefore, pollutants emitted during the production of HMAM have a significant negative impact on regional air quality (Almeida and Picado, 2023; Iwanski et al., 2023).

In this background, the warm mix technology of asphalt pavement materials came into being. As an environmentally friendly road material production technology, it provides an effective way to solve the environmental problems of traditional HMAM technology. Asphalt pavement material warm mixing technology mainly includes machine additive method, chemical process method and foam process method three categories (Qin et al., 2010; Xu et al., 2020; Ozturk and Kutay, 2014). The first two kinds of warm mixing technology started earlier in China, and has been applied to a certain scale, represented by the organic additive Sasobit and surfactant Evotherm. Mechanical foaming warm mixing technology started relatively late, but the cost is low, and gradually received attention. The basic principle of asphalt and trace water in the mechanical foaming device mixed to form foam asphalt, by increasing the asphalt surface area, reduce the asphalt viscosity, to achieve uniform mixing of asphalt and minerals at relatively low temperatures. It also enhances the ease of workability of bituminous mixtures and ultimately improves the compactability of the pavement (You et al., 2017; Song et al., 2015; Bairgi et al., 2018). The strategy cuts the mixture construction process temperature by 10°C–30°C and, meanwhile, cuts asphalt fumes and CO2 emissions by more than 80% and 50% respectively, in contrast to the typical HMAM (Qin et al., 2009).

Zhu studied the change law of voidage of FWMAM under different mixing temperatures and compaction temperatures. It was found that the mixing and compaction temperatures of FWMAM could be reduced by 20°C–30°C compared to HAM (Zhu et al., 2014). Bairgi concluded that the foaming process of asphalt reduces the friction value which helps the asphalt to coat the aggregate surface and improves the mobility of the asphalt between the aggregates at lower compaction temperatures (Bairgi et al., 2019). With the development of modern phase testing technology, road science and technology workers try to explore the technical characteristics of foam asphalt from a more microscopic level. Wen found that foam warm-mix asphalt mastic has better thermal stability than matrix asphalt mastic by using differential scanning calorimeter study (Wen et al., 2020). Qtaish studied the micromechanical properties of foam warm mix asphalt using atomic force microscopy and found that its aging resistance is comparable to that of hot mix asphalt (Abu et al., 2018). Hande proposed a method for evaluating the foaming effect of asphalt based on image processing techniques, and the foam size index can evaluate the working characteristics of foamed asphalt more effectively (Hande and Ozturk, 2018). Wei analyzed the surface free energy of foam asphalt with mineral at different stages and proposed for an assessment of the capacity to resist against water damage of FWMAM by the comparison between the adhesion work and the stripping work (Wei et al., 2017).

However, the technology faces key bottlenecks in its practical application. Specifically, the mechanism by which the amount of foamed water affects the mechanical properties of mixes has not been clarified, leading to large fluctuations in performance and a lack of design criteria. For example, while excess foamed water may improve asphalt fluidity, the residual water may weaken asphalt-aggregate interface adhesion and trigger water damage. Insufficient foamed water, on the other hand, does not sufficiently reduce construction temperatures and diminishes environmental benefits.

To summarize, there have been a lot of achievements at home and abroad on the working mechanism, composition design and performance evaluation of foam warm mix asphalt mixtures, which have promoted the application of this technology, but there are still some concerns in the industry. The water usually weakens the coating of bitumen on the mineral surface and substantially reduces the asphalt mixture's performance on the road, so water-induced diseases of the asphalt road surface have become one of the major problems in road engineering.

Specifically, the effect of water on the performance of FWMAM is one of the most important concerns for this technology because of the actively injected water. Zou investigated the phase change and dissipation of moisture in FWMAM at various stages of construction using indoor simulation tests and found that the internal structural moisture gradually decreased with the construction process (Zou et al., 2016). Wang found that the viscosity of foam warm mix asphalt has a better sensitivity to the amount of water used for foaming (Wang and Liu, 2017). Arega studied the foaming and breaking process of asphalt using laser and ultrasonic rangefinders and found that moisture level dramatically influences the foam asphalt quality (Arega et al., 2013). Many studies have been carried out at home and abroad on the mechanism of foaming water consumption on asphalt, but the influence on the mixture of foaming water consumption has rarely been reported (Zhou et al., 2021; Fan et al., 2024). At the same time, the quantitative relationship between the amount of foamed water and the mechanical properties of the mix (water loss resistance, dynamic modulus, fatigue life) has not been fully revealed. The existing asphalt foaming water consumption is depended largely on the asphalt foaming parameters, without fully considering the properties in the mixture, which is the key factor that ultimately determines the quality of the pavement (Abdelsalam et al., 2020; Sun et al., 2024). However, all of the above studies also correlate the amount of foamed water with the mechanical properties of the mixture.

Therefore, this paper comprehensively tested the mechanical properties of FWMAM and FWMAM-SBS under different foaming water consumption conditions, including water damage resistance, rutting resistance, anti-temperature cracking resistance, dynamic viscoelasticity characteristics and anti-fatigue performance. And it analyzed the change rule of FWMAM and FWMAM-SBS performance indexes under different working conditions. As a comparison, controlled tests were conducted on HMAM and HMAM-SBS. The aim of the study was to investigate a mechanism of implication in foaming water consumption on mechanical behaviour of FWMAM and FWMAM-SBS, and to give a guide to optimize the design of foaming water consumption of FWMAM and FWMAM-SBS. This achievement not only provides a reliable basis for the large-scale application of warm mix foam asphalt technology in green road engineering, responding to the global demand for low-carbon infrastructure development. At the same time, it also provides theoretical support for the engineering application of green and low-carbon pavement

TABLE 1 Asphalt technical indicators.

Indicator		Matrix asphalt	Modified asphalt
25° C Needle penetration/0.1 mm		70	57
135°C kinematic viscosity/Pa.s		—	1.0
Softening point/°C		51.5	61.5
Ductility/cm (15 °C)		>100	—
Ductility/cm (5 °C)		—	24
Residue after TFOT	Mass loss/%	0.17	0.30
	25° C residual needle penetration ratio/%	66	65
	Ductility/cm (15 °C)	27	—
	Ductility/cm (5 °C)	—	17

TABLE 2 Gradation of aggregate.

Gradation	Passage rate of various sieve holes/%										
	19	16	13.2	9.5	4.75	2.36	1.18	0.6	0.3	0.15	0.075
AC-16C	100.0	98.5	90.8	75.2	46.4	25.0	15.0	10.6	8.3	6.5	5.5

TABLE 3 Fine aggregate test results.

Test indicators	Unit	Measured value
Apparent Relative Density	-	2.711
Sand Equivalent	%	72
Angularity (Flow Time)	s	34

materials and helps the sustainable development of transportation infrastructure.

2 Raw material

In this study, two types of asphalt were selected. These parameters' technical details are systematically presented in Table 1.

The same mineral gradation was used for both the WMAM and the HMAM, as shown in Table 2, and the ratios of oil and stone were both 4.8%. The test results of coarse aggregates and fine aggregates are shown in Tables 3, 4.

3 Test scheme

The foaming temperatures of matrix asphalt and modified asphalt were 150°C and 160°C, respectively. The water consumption for foaming is 1%, 2% and 3% for both types of asphalt (Guo et al., 2020; Alnadish et al., 2021). The range of water content allows the asphalt to achieve a better expansion rate, resulting in a lower transient viscosity and better workability. If the water content is too high, it will lead to too much water in the foam asphalt, the foam stability is poor, and easy to rupture, which affects the use effect. If the water content is too low, the water vapor cannot be generated sufficiently, the asphalt expansion is insufficient, the viscosity reduction is not obvious, and it is not conducive to the wrapping with the aggregate.

The foaming equipment was the Wirtgen asphalt foaming equipment, as shown in Figure 1. The foaming method refers to JTG/T 5521–2019 specification. The foaming measurement is shown in Table 5. The aggregate heating temperature was 170°C, and the forming temperature of FWMAM and HMAM specimens was 130°C and 145°C, respectively. The forming temperatures of FWMAM-SBS samples were 150°C and 165°C, respectively. Where, FWMAM/1% represents FWMAM with 1% foaming water consumption, FWMAM-SBS/1% represents FWMAM-SBS with 1% foaming water consumption. The latter situation is analogous. The research flowchart is shown in Figure 2.

3.1 Water damage resistance test scheme

The immersion Marshall strength and freeze-thaw split strength tests are used to analyze the changing law of water damage resistance of FWMAM under different foaming water consumption conditions (Liu et al., 2020). The test

TABLE 4 Coarse aggregate test results.

Test indicators	Unit	Measured value	
		4.75–9.5 mm	9.5–19 mm
Apparent relative density	-	2.738	2.730
Water absorption	%	0.60	0.38
Content of particles finer than 0.075 mm	%	0.5	0.4
Soft particle content	%	-	
Los angeles abrasion loss	%	27.4	24.0
Aggregate crushing value	%	-	22.3
Boiling water stripping test	Level	-	4
Soundness of aggregate	%	-	

FIGURE 1
The wirtgen asphalt foaming equipment.

method was referred to the current Test Regulations for Highway Engineering Asphalt and Asphalt Mixture (JTG E20-2011) (Ministry of Transport of the People's Republic of China, 2011). Every set of tests was repeated five times, and the average value was taken as the final result after removing outliers.

3.2 Rutting resistance test scheme

The uniaxial penetration strength test can be used to characterize the shear properties of asphalt mixtures. So, the test is used to analyze the effect of foaming water consumption on the rutting resistance of FWMAM. The cylindrical specimen φ150 × 105 mm was prepared by rotary compactor, and then the core was cut into φ100 × 100 mm test specimen. The voidage of the specimen is controlled in the range of 7% ± 0.5%. The loading rate was 1 mm/min, the loading head diameter was 28.5mm, and the test temperature was 60°C (Hu et al., 2022). The test was repeated 3 times for every group and the average value was taken as the final result. The penetration strength can be calculated from Formula 1, 2:

$$R_T = f_T \sigma_p \tag{1}$$

$$\sigma_p = P/A \tag{2}$$

Where: R_T is the penetration strength (MPa); σ_p is the penetration stress (MPa); P is the peak load (N); A is the contact area between the loading head and the specimen (mm^2); f_T is the penetration stress factor, 0.34.

3.3 Low temperature performance test scheme

The stress distribution state of the loading process of the semi-circular bending (SCB) test is closer to actual pavement (Wang et al., 2020). Therefore, the SCB test was used to assess the impact in foaming water consumption on the low-temperature performance of FWMAM. Firstly, the cylindrical specimen of φ150 × 105 mm is prepared by rotary compactor, and then it is cut into semi-circular specimens of 150 mm in diameter and 50 mm in height for testing. The specimen was pre-cut with a seam depth of 15 mm and the void ratio of the specimen was 7% ± 0.5%. Every set of tests was repeated three times. The distribution of the specimen's bottom two support points was 120 mm, and the test conditions were −24°C, −12°C, and 0°C. The breaking energy (G_f) is calculated from Formula 3, 4.

$$W_f = \int P du \tag{3}$$

$$G_f = W_f/(r-a) \times t \tag{4}$$

Where: G_f is the breaking energy of the specimen (J/m^2); P is the applied load (kN); u is the displacement corresponding to P (mm); r, t and a are the radius, thickness and precut seam depth of the specimen respectively, (m).

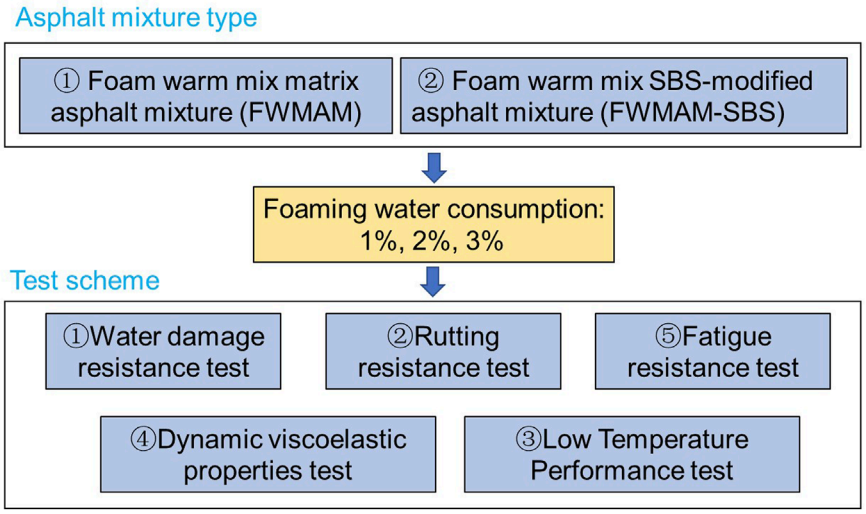

FIGURE 2
The research flowchart.

TABLE 5 The results of foamed asphalt.

Foaming water/%	Expansion rate/times		Half-life/s	
	Matrix asphalt	Modified asphalt	Matrix asphalt	Modified asphalt
1	12	5	14	>300
2	19	6	6	>300
3	26	6	5	>300

TABLE 6 The number of loading cycles of dynamic modulus test.

Load frequency/Hz	Number of times the load reloaded
25	200
10	200
5	100
1	20
0.5	15
0.1	15

TABLE 7 Dynamic modulus test load level (kPa).

Temperature	Load frequency/Hz					
	0.1	0.5	1	5	10	25
4°C	700	840	980	1,120	1,260	1,400
20°C	350	420	490	560	630	700
40°C	142	162	184	206	228	250

3.4 Dynamic viscoelastic properties test scheme

The dynamic modulus was used as an evaluation index to explore the implication of foaming water consumption on the dynamic viscoelastic properties of FWMAM. The AMPT equipment was used for the test. And, the cylindrical specimen φ150 × 170 mm was prepared by rotary compactor, and the core was drilled and cut into φ100 × 150 mm test specimen. The voidage of the specimen was controlled within 7% ± 0.5%. The test temperature is 4°C, 20°C, 40°C, the load is the offset sine wave, the load frequency is 25Hz–0.1 Hz. Repeat the test 5 times for every group and take the average value as the final result. The number of repetitive loadings and load levels for the dynamic modulus tests are shown in Tables 5–7.

In accordance with time-temperature equivalent principle, the main curve can be constructed in a wide frequency domain under certain temperature conditions through the

TABLE 8 Immersion marshall test results of mixtures.

Type of mixture	Stability/kN	Variation coefficient/%	Immersion stability/kN	Variation coefficient/%	Residual stability/%	Variation coefficient/%
HMAM	11.55	3.5	10.0	3.7	87.0	4.1
FWMAM/1%	10.01	3.8	9.51	3.3	95.0	3.5
FWMAM/2%	10.34	2.5	9.31	3.7	90.0	3.7
FWMAM/3%	10.01	4.7	9.05	2.2	90.4	4.7
HMAM-SBS	12.06	3.7	11.08	3.6	92.0	2.7
FWMAM-SBS/1%	11.86	4.7	11.29	4.2	95.2	4.9
FWMAM-SBS/2%	11.90	1.0	11.28	3.8	94.8	3.8
FWMAM-SBS/3%	10.77	4.2	10.74	3.1	99.0	4.6

limited dynamic modulus test results (Khosravifar et al., 2015). For nonlinear fitting based on Sigmoidal function, in Formula 5.

$$log|E^*| = \delta + \frac{\alpha}{1 + EXP(\beta + \gamma(log(f_r))} \quad (5)$$

Where, $|E^*|$ is the dynamic modulus (MPa); f_r is the scaling frequency (Hz); and δ, α, β, γ are the fitting parameters.

The temperature displacement factor is the amount of shift required to bring the viscoelastic data curves at different temperatures into complete coincidence on the master curve at the reference temperature by horizontally translating the curves. Therefore, the temperature shift factor is an important bridge between temperature and time scales. The expression for the temperature shift factor is given in Formula 6.

$$\log(f_r) = \log(a(T)) + \log(f) \quad (6)$$

Where, $\alpha(T)$ is the displacement factor, and f is the frequency, (Hz).

On this basis,the temperature displacement factor is calculated from Formula 7 based on the Arrhenius time-temperature equivalence principle (Ghabchi et al., 2016).

$$\log(a(T)) = c\left(\frac{1}{T_k} - \frac{1}{T_{ref}}\right) \quad (7)$$

Where, T_k is temperature; T_{ref} is the main curve temperature; and c is the fitting parameter.

From Formula 5–7, the parameters of the master curve can be obtained using the least squares fitting method.

3.5 Fatigue resistance test scheme

To determine the fatigue performance of FWMAM under various conditions of foaming water consumption by four-point bending fatigue test using the number of loadings as the evaluation index. The test method was referred to the AASHTO T321-03 standard, and the offset sine wave was used as the standard loading waveform of fatigue test (American Association of State Highway and Transportation Officials AASHTO, 2003). The specimens were formed by shear compactor. The void ratio of the specimen was 7% ± 0.5%, and the ambient temperature of the test is 15°C. The load rate is 10 Hz and strain control was used. The bending stiffness modulus corresponding to the 50th loading is taken as the initial value. The test was stopped when modulus of strength of the mix decayed to half of the initial value. The tests were repeated five times for every group, and the average value was taken as the final result after removing the outliers.

4 Results and discussion

4.1 Water damage resistance performance

The test results of water damage resistance of FWMAM and HMAM are shown in Table 8, 9.

In Table 8, 9, from the matrix asphalt results, when foaming water consumption is less than 2%, the residual stability and TSR of FWMAM are slightly higher than HMAM, indicating that FWMAM has slightly better water damage resistance than HMAM. It is speculated that the primary cause of this is the expansion rate of matrix asphalt after foaming is higher (≥8 times). This enhances the wrapping of the asphalt around the aggregate and improves the cohesion of the asphalt to the aggregate. This improves the performance of the mixture in aqueous environments. However, when the foaming water usage is large, the excess amount of water will rather reduce the adherence of bitumen to the aggregate, which will influence the mixture's water stability.

In the case of modified asphalt, the residual stability of FWMAM-SBS was higher than that of HMAM-SBS, and the TSR was slightly lower than that of HMAM-SBS. In contrast to the matrix asphalt, the increase in foaming water consumption does not continue to reduce the FWMAM-SBS water stability, which is

TABLE 9 Freeze-thaw splitting strength test results of mixtures.

Type of mixture	Splitting strength/MPa	Variation coefficient/%	Freeze-thaw splitting strength/MPa	Variation coefficient/%	Tensile strength ratio (TSR)/%	Variation coefficient/%
HMAM	0.72	3.7	0.53	3.3	73.6	3.7
FWMAM/1%	0.85	3.9	0.63	5.1	74.1	2.7
FWMAM/2%	0.78	5.8	0.60	2.2	76.9	2.7
FWMAM/3%	0.75	3.7	0.55	3.8	73.3	5.0
HMAM-SBS	0.98	5.0	0.81	4.2	82.7	2.8
FWMAM-SBS/1%	1.01	2.1	0.79	3.8	78.2	5.2
FWMAM-SBS/2%	0.99	3.9	0.78	5.6	78.8	3.8
FWMAM-SBS/3%	0.96	3.8	0.76	2.8	79.2	2.8

TABLE 10 Uniaxial penetration strength test results of HMAM and FWMAM.

Type of mixture	Penetration stress/MPa	Variation coefficient/%	Penetration depth/mm	Variation coefficient/%	Penetration strength/MPa	Variation coefficient/%
HMAM	1.79	3.2	1.514	3.2	0.61	4.3
FWMAM/1%	1.88	3.5	1.347	4.5	0.64	2.9
FWMAM/2%	2.11	4.6	1.258	4.6	0.72	2.5
FWMAM/3%	2.24	4.2	1.223	3.2	0.76	4.6

TABLE 11 Uniaxial penetration strength test results of HMAM-SBS and FWMAM-SBS.

Type of mixture	Penetration stress/MPa	Variation coefficient/%	Penetration depth/mm	Variation coefficient/%	Penetration strength/MPa	Variation coefficient/%
HMAM -SBS	2.15	4.2	1.234	4.5	0.73	3.5
FWMAM-SBS/1%	2.02	4.2	1.367	4.2	0.69	3.3
FWMAM-SBS/2%	1.98	4.1	1.385	3.7	0.67	3.6
FWMAM-SBS/3%	2.06	4.3	1.312	3.8	0.70	4.2

associated with excellent adherence and deformation resistance of modified asphalt.

In summary, FWMAM water stability is basically comparable to that of HMAM for matrix asphalt at 1%–3% foaming water consumption. And even slightly higher than HMAM at lower foaming water requirements. To control the water stability of FWMAM, the water consumption of foaming should be controlled as low as possible under the condition of meeting the foaming parameters of asphalt. For SBS modified asphalt, in various foaming water consumption conditions, it is found that the water stability of FWMAM-SBS is not obviously changed, and the water damage resistance performance is low susceptibility to the change of foaming water consumption.

4.2 Rutting resistance performance

The single-axial penetration strength test results of FWMAM and FWMAM-SBS under different foaming water consumption are shown in Tables 10, 11.

From Table 10, the FWMAM has greater penetration stress and penetration strength than HMAM. However, the depth of penetration is less than that of the HMAM, which is related to the enhancement of adhesion of foamed asphalt and aggregate. For example, at 3% consumption of foaming water, the penetration strength of FWMAM is increased by 24% compared with HMAM. It is shown that the rutting resistance of FWMAM is more superior than the performance of HMAM. And under the

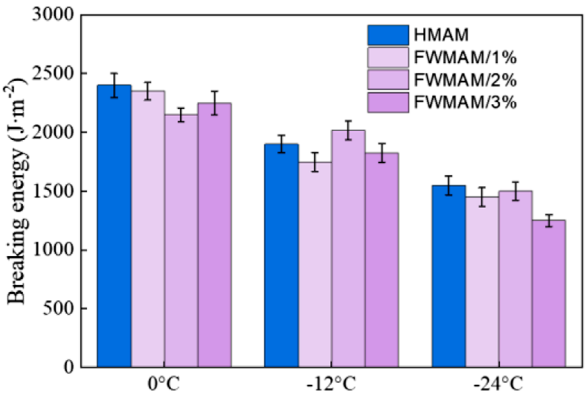

FIGURE 3
SCB test results of HMAM and FWMAM.

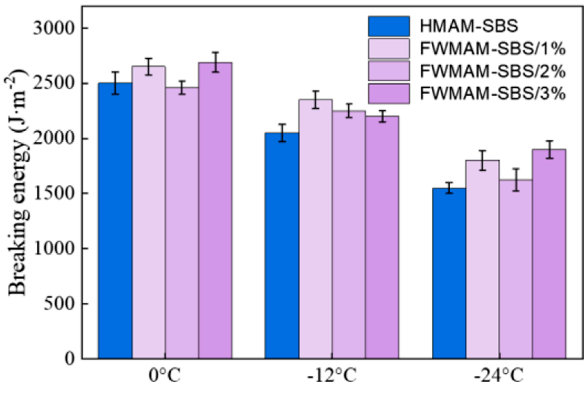

FIGURE 4
SCB test results of HMAM-SBS and FWMAM-SBS.

condition of certain foaming water requirement, more foaming water requirement corresponds to stronger rutting resistance.

For FWMAM-SBS in Table 11, the penetration stress and penetration strength are slightly less than those of HMAM-SBS. This shows a slight degradation of the high-temperature deformation capacity of FWMAM-SBS compared to that of HMAM. However, there was no consistent pattern of change with the increase in foaming water quantity. When comparing FWMAM and FWMAM-SBS, the SBS-modified asphalt is more stable to resist heat deformation due to the formation of a more stable colloidal structure than that of the matrix asphalt, which makes the deformation capacity to FWMAM-SBS less affected by the change in foaming water consumption.

4.3 Low temperature cracking resistance performance

The SCB breaking energy results of FWMAM and FWMAM-SBS under different foaming water conditions are shown in Figures 3, 4.

From Figures 3, 4, it can be seen that in an identical temperature condition, the breaking energy of FWMAM and FWMAM-SBS has no obvious change rule when the water used for foaming is increased. However, as the temperature decreases, the fracture energy gradually decreases, showing the variation in temperature has a greater impact in the cracking resistance of the foam warm mixture. In the case of modified asphalt, the breaking energy of FWMAM-SBS is basically larger as compared with that of HMAM-SBS, indicating that FWMAM-SBS has better cracking resistance than HMAM-SBS under low temperature environment. For matrix asphalt, the overall fracture energy of FWMAM is smaller than that of FWMAM. When the foaming water consumption is 1%, the difference between FWMAM and HMAM in anti-cracking performance at low temperature is relatively small. In Table 12, the mean values and coefficients of variation of the fracture energy of the FWMAM based on the three foaming water volumes are presented at different temperature conditions.

In Table 12, the effect of variation in foaming water consumption on the fracture energy of FWMAM and FWMAM-SBS is enhanced with decreasing temperature. This demonstrates that the variability of the low-temperature crack resistance in FWMAM and FWMAM-SBS becomes larger under different foaming water consumption conditions. Therefore, when applying foam warm mix asphalt mixtures in the cold regions in the north of China, the amount of water used for foaming determined by design should be strictly controlled in order to ensure the stability of low-temperature performance.

The phenomenon of decreasing fracture energy with decreasing temperature is closely related to the viscoelastic properties of asphalt. The brittleness of asphalt gradually increases at low temperatures, which makes the possibility of stress concentration within the mix gradually increase, thereby making it more susceptible to crack propagation and decreasing the fracture energy. At the same time, the trace amount of incompletely evaporated moisture may also form ice crystals at the interface, exacerbating the low-temperature cracking susceptibility, which may originate from the weakening effect of the residual moisture on the asphalt-aggregate interface, and therefore, moisture may also have some effect on the fracture energy. Superimposed on the viscoelastic properties of asphalt, this ultimately results in differences in fracture energy at different temperatures.

4.4 Dynamic viscoelastic performance

The dynamic modulus master curves of foam FWMAM and HMAM are shown in Figures 5, 6, respectively. The reference temperature for the master dynamic modulus curve is 20°C. The fitted parameters for all master curves have been listed in full in Table 13.

From Figures 5, 6, at different foaming water requirements, the dynamic modulus of FWMAM is consistent with that of HMAM, with an overall S-shaped flattened curve. It is shown that the viscoelastic behaviour in FWMAM is not similar to that in HMAM, and that the change in the amount of water used for foaming does not change this property. The dynamic modulus of FWMAM is essentially the same as that of HMAM under extreme low-frequency loading. This property is not varied by changes in the amount

TABLE 12 Average value and coefficient of variation of fracture energy of FWMAM and FWMAM-SBS.

Type of mixture	Temperature/°C	Mean/J·m^{-2}	Variation coefficient/%
FWMAM	0	2,164	4.1
	−12	1852	4.9
	−24	1,349	7.3
FWMAM-SBS	0	2,577	3.4
	−12	2,349	3.8
	−24	1788	7.4

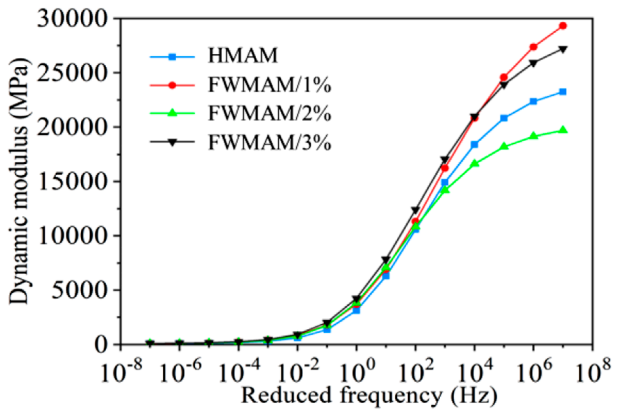

FIGURE 5
The master curve of HMAM and FWMAM.

TABLE 13 The fitted parameters for all master curves.

Type of mixture	δ	α	β	γ	R^2
FWMAM/1%	2.1	4.3	−0.7	1.2	0.98
FWMAM/2%	2.0	4.5	−0.6	1.1	0.97
FWMAM/3%	1.9	4.6	−0.5	1.0	0.96
FWMAM-SBS/1%	2.3	4.0	−0.5	1.0	0.96
FWMAM-SBS/2%	2.4	3.9	−0.4	0.9	0.95
FWMAM-SBS/3%	2.2	4.1	−0.6	1.1	0.94
HMAM	2.2	4.2	−0.8	1.3	0.98
HMAM-SBS	2.4	3.9	−0.4	0.9	0.95

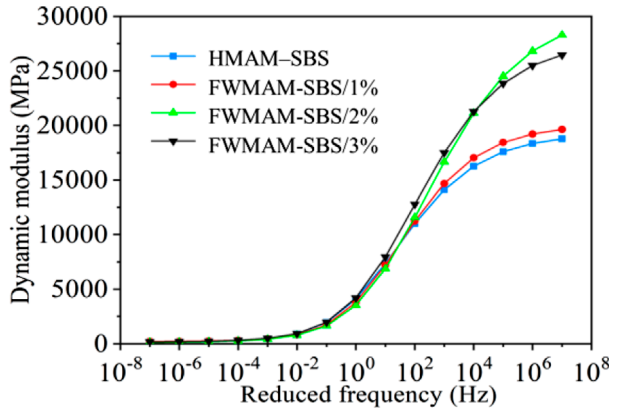

FIGURE 6
The master curve of HMAM SBS and FWMAM-SBS.

of water used for foaming. The dynamic modulus of FWMAM is essentially the same as that of HMAM under extreme low-frequency loading. As the loading frequency grows, there is an increase in effectiveness of impact of various water requirements for foaming on the mixture's dynamic modulus. The higher the water requirement for foaming, a higher dynamic modulus of mixture can be achieved within a certain loading interval. However, when the loading frequency becomes larger to a degree, the main curve crosses, and the water requirement and dynamic modulus do not show a consistent rule of change.

The FWMAM dynamic modulus is consistently greater than the HMAM in the conventional loading frequency interval of 0.1–25 Hz. And the higher the water consumption for foaming, the higher the dynamic modulus. It is shown that the strength of FWMAM is better than that of HMAM at different foaming water levels. This is related to the increased adhesion of the foam asphalt and aggregates and the increased resistance to deformation. For FWMAM-SBS, the dynamic modulus of FWMAM-SBS was not significantly changed from that of HMAM-SBS at 1%–3% foaming water consumption. Mainly because modified asphalt is more structurally stable than matrix asphalt, less affected by external factors. Therefore, for FWMAM, the foaming water consumption has a positive correlation with its strength, while for FWMAM-SBS, the foaming water consumption has no significant effect on its strength.

It is worth noting that when water content changes, the dependence of dynamic modulus on frequency appears fuzzy at higher frequency values. Specifically, the maximum value of FWMAM is 1% and the maximum value of FWMAM-SBS is 2%.

TABLE 14 Fatigue resistance results in differernt mixtures.

Type of mixture	Strain/με	Fatigue life/times	Fatigue life ratio of warm mix to hot mix
HMAM	80	1072086	-
	100	216,661	-
	200	6,822	-
FWMAM/1%	80	1,430,574	1.33
	100	297,834	1.37
	200	8,138	1.19
FWMAM/2%	80	1,295,429	1.21
	100	286,749	1.32
	200	7,051	1.03
FWMAM/3%	80	1,278,652	1.19
	100	226,804	1.05
	200	7,431	1.09
HMAM-SBS	100	796,064	-
	200	29,701	-
	300	7,285	-
FWMAM-SBS/1%	100	921,534	1.16
	200	33,087	1.11
	300	7,892	1.08
FWMAM-SBS/2%	100	994,283	1.25
	200	35,964	1.21
	300	8,154	1.12
FWMAM-SBS/3%	100	974,165	1.22
	200	30,658	1.03
	300	7,691	1.06

The reasons are speculated as follows: The 1% foaming water can fully foam the asphalt (12 times expansion rate in Table 5), forming a uniform foam structure and enhancing the adhesion between asphalt and aggregate. Under high-frequency loading (short-time loading), the elastic response is dominant, and the well-dispersed asphalt binder phase can transfer the stress more efficiently, thus enhancing the dynamic modulus.

SBS would form a three-dimensional elastic network in the asphalt, and the 2% foaming water could promote asphalt foaming without destroying the polymer structure. However, the 1% foaming water may not fully activate the foaming potential of SBS-modified asphalt (the modified asphalt expansion rate is only 5–6 times in Table 5), while the 3% foaming water may lead to localized moisture aggregation, which interferes with the continuity of the SBS network, thus reducing the dynamic modulus. Therefore, matrix asphalt and SBS-modified asphalt showed some differences.

4.5 Fatigue resistance performance

The fatigue test results for HMAM and FWMAM are illustrated in Table 14.

As shown in Table 14, the number of fatigue life times of FWMAM with foam is greater than HMAM under different foaming water consumption conditions for both two asphalts. The

TABLE 15 Regression results of fatigue resistance of mixtures.

Type of mixture	n	k	R^2
HMAM	0.017	7.250	0.98
FWMAM/1%	0.018	7.424	0.98
FWMAM/2%	0.018	7.416	0.98
FWMAM/3%	0.017	7.316	0.97
HMAM-SBS	0.010	6.784	0.95
FWMAM-SBS/1%	0.010	6.861	0.98
FWMAM-SBS/2%	0.010	6.908	0.95
FWMAM-SBS/3%	0.011	6.889	0.95

fatigue resistance of FWMAM is improved compared to HMAM. This is mainly due to the lower mix production temperature, which reduces the degree of asphalt aging and allows the mix to provide improved resistance to elastic deformation under repetitive loading. The difference in fatigue life between FWMAM and HMAM is significant at lower strain levels. In summary, the fatigue performance of FWMAM is roughly 1.2 times higher than that of HMAM at strain levels less than 100 με for 1%–3% foaming water use. After raising the strain level, the difference in fatigue lifetimes of the two mixes gradually decreases. As the amount of water used for foaming rises, the overall fatigue life of FWMAM decreases gradually for matrix asphalt. In addtion, the life of FWMAM-SBS initially grows and then declines, and the fatigue life of FWMAM-SBS achieves its greatest fatigue life at 2% of foaming water consumption.

Table 15 shows the fitting results of fatigue test data of HMAM and FWMAM, HMAM -SBS and FWMAM-SBS by using fatigue Equation 8.

$$\log(N_r) = k - n\sigma \tag{8}$$

Where: N_f is the number of fatigue life; σ is the strain; n and k are the parameters.

From Table 15, at 1%–3% of foaming water requirement, the fitting curve determination coefficient R^2 of FWMAM and FWMAM-SBS fatigue equation is high, and the fatigue life of FWMAM within a certain foaming water consumption range can be predicted by using this fatigue equation. For the fatigue equation, a larger n indicates a greater sensitivity to the change in fatigue life of the mix relative at the change in its strain level, i.e., a greater risk of fatigue cracking. For the same type of asphalt, there is basically no change in the n-value of the FWMAM and HMAM at 1%–3% foaming water consumption. This suggests that the sensitivity of FWMAM and HMAM, FWMAM-SBS and HMAM-SBS fatigue lives to strain changes is close. And, the FWMAM and FWMAM-SBS have better fatigue resistance. In comparison, the FWMAM-SBS is less susceptible to strain than that of FWMAM, which is mainly due to the fact that SBS-modified asphalt forms a more developed spatial mesh cross-linking structural system than matrix asphalt, which has more excellent deformation resistance.

5 Correlation and mechanism analysis

5.1 Correlation analysis

Based on the experimental data above, this paper used Pearson's phase relationship to quantify the relationship between foaming water dosage and key performance indicators, and the results are as follows in Table 16.

The TSR of FWMAM was significantly negatively correlated with the amount of foamed water, indicating that excessive foamed water (>2%) weakens the water stability of asphalt mixtures, which is consistent with the decreasing trend of TSR of FWMAM. The insignificant change in TSR of FWMAM-SBS is attributed to the suppression of water penetration by the SBS network and the reduced risk of interfacial weakening.

The rutting strength of FWMAM is strongly and positively correlated with the amount of foamed water, and the increase in foamed water enhances asphalt mobility (expansion from 12 to 26 times) and promotes uniform coating of the aggregate surface. FWMAM-SBS is insensitive to foamed water due to SBS network enhanced elastic recovery and rutting resistance.

The fracture energy of FWMAM is significantly negatively correlated with foamed water, and excess water may remain to form ice crystal micropores, which become low-temperature crack sprouting points. FWMAM-SBS has less performance fluctuation due to energy absorption by plastic deformation of SBS.

The dynamic modulus of FWMAM is positively correlated with the foamed water at 10 Hz, which enhances asphalt dispersion and expansion and strengthens the high-frequency elastic response, resulting in a rightward shift of the main curve. FWMAM-SBS has low sensitivity of modulus to foaming water due to inhibition of viscous flow by SBS network. The negative correlation of fatigue life reflects the fact that excess foamed water accelerates asphalt deterioration, leading to reduced durability.

5.2 Mechanism analysis

In terms of water damage properties, foamed water increase initially (≤2%) enhances asphalt encapsulation of aggregates by boosting the expansion rate (Table 3), but there may be excess water residue to form a weak interfacial layer, leading to a decrease in TSR. And the three-dimensional network inside SBS-modified asphalt may hinder water penetration and effectively reduce the degree of interface weakening. In terms of rutting resistance foamed water increases asphalt fluidity, promotes uniform film formation, and enhances the thickness of the asphalt film between aggregates, thereby increasing shear strength. The elastic network within the SBS-modified asphalt provides a sustained resilience that counteracts the negative effects of moisture on viscoelasticity.

In terms of low temperature performance, the brittleness of asphalt increases at low temperatures, and the micropores that may be formed by the residual foaming water become the crack initiation point, and the fracture energy decreases gradually with the increase of foaming water. And the network plasticity of SBS modified asphalt

TABLE 16 Calculation of pearson's correlation coefficient between indicators and water consumption.

Performance	Mixture type	Pearson correlation coefficient R	P Value	Significance
Water damage resistance Performance	FWMAM	−0.75	0.02	Significant negative correlation
	FWMAM-SBS	−0.32	0.45	insignificant
Rutting resistance Performance	FWMAM	0.92	0.001	significant positive correlation
	FWMAM-SBS	0.35	0.38	insignificant
Low Temperature Performance	FWMAM	−0.76	0.01	Significant negative correlation
	FWMAM-SBS	−0.41	0.25	insignificant
Dynamic modulus	FWMAM	0.85	0.001	significant positive correlation
	FWMAM-SBS	0.28	0.42	insignificant
Fatigue resistance Performance	FWMAM	−0.85	0.001	Significant negative correlation
	FWMAM-SBS	0.78	0.03	significant positive correlation

will absorb the fracture energy and reduce the crack extension rate. Regarding the dynamic modulus, the increase in foamed water enhances the asphalt dispersion (Table 3 expansion rate) and strengthens the elastic response (increase in modulus in the high frequency band of the main curve), but the excess water retention leads to an increase in viscous dissipation (increase in phase angle). In contrast, SBS-modified asphalt possesses a network structure that inhibits viscous flow and reduces modulus sensitivity to foamed water. In terms of fatigue performance, a moderate amount of foamed water (1%) reduces asphalt aging and delays microcrack initiation; excessive foamed water (>2%) leads to an increase in interfacial defects, accelerating the accumulation of fatigue damage, and the network within the SBS modified asphalt prevents also crack expansion.

The interaction between foamed water and SBS modified asphalt is a dynamic balance: appropriate amount of foamed water enhances the aggregate encapsulation and rutting resistance by improving asphalt mobility and expansion rate, but its residual water is prone to induce interfacial weakening, low-temperature microporous brittleness, and excessive viscous dissipation. The SBS three-dimensional elastic network effectively counteracts these negative effects by blocking water penetration, absorbing fracture energy and inhibiting crack extension, while maintaining dynamic modulus stability through viscoelastic recovery.

6 Conclusion

The performance evolution of FWMAM and FWMAM-SBS was compared under the condition of 1%–3% foaming water consumption by using water damage performance, dynamic viscoelasticity characteristics, fatigue resistance and so on as evaluation systems. The conclusions are as follows.

(1) The performance of water damage prevention of FWMAM is basically at the same level with HMAM, and the performance of water damage prevention of FWMAM is even slightly better than HMAM in the case of lower foaming water consumption (less than 2%). The ratio of freezing-thaw split strength ratio is not significantly different for FWMAM-SBS but lower than that of HMAM-SBS.

(2) The rutting resistance of FWMAM is stronger than that of HMAM, and the higher the water consumption of foaming, the better the rutting resistance. The anti-rutting performance for FWMAM-SBS is marginally decreased compared to HMAM-SBS, and is less affected by the change in foaming water consumption.

(3) The resistance to low-temperature cracking of FWMAM is less than the resistance of HMAM, when the water used for foaming is 1%, the difference between the two is relatively small. The performance of FWMAM-SBS is basically better than that of HMAM-SBS, but as the decline of temperature, the influence of the change of foaming water consumption to low-temperature performance of FWMAM and FWMAM-SBS is enhanced.

(4) The characteristics of the variation to the master curve in FWMAM are consistent with those of HMAM. Water consumption for foaming is positively correlated with strength in FWMAM and is better than HMAM at conventional loading frequencies. But it has no significant effect on the strength of FWMAM-SBS.

(5) The anti-fatigue properties for FWMAM and FWMAM-SBS are superior to those of the corresponding HMAM. The fatigue life of FWMAM decreases in general as the foaming water consumption increases, and the fatigue life in FWMAM-SBS firstly grows and subsequently declines, and peaks at 2% foaming water consumption. The FWMAM-SBS fatigue life is less sensitive to strain than FWMAM.

As a combination of asphalt foaming performance and asphalt mixtures of various road performance, matrix asphalt foaming water should not be more than 1%. And, the amount of water

used for foaming SBS-modified asphalt should not exceed 2%. The above conclusions are based on a limited number of samples, and more generalized conclusions would require the selection of more different types of asphalt to be analyzed in comparative tests.

Data availability statement

The original contributions presented in the study are included in the article/supplementary material, further inquiries can be directed to the corresponding author.

Author contributions

YH: Writing – original draft, Writing – review and editing. HL: Data curation, Methodology, Writing – review and editing. CH: Investigation, Methodology, Writing – review and editing. YZ: Conceptualization, Data curation, Writing – review and editing. PW: Formal analysis, Validation, Visualization, Writing – review and editing. PL: Investigation, Software, Writing – review and editing.

Funding

The author(s) declare that financial support was received for the research and/or publication of this article. The authors would like to thank Guangxi development key research program (Development of a High-Precision Intelligent Simulation and Active Prevention Cloud Platform for the Service Performance of Asphalt Pavements on Coastal Hot and Humid Highways, Grant No. GuikeAB22080091). Their assistance is sincerely appreciated.

Acknowledgments

The authors would like to thank Guangxi development key research program (Development of a High-Precision Intelligent Simulation and Active Prevention Cloud Platform for the Service Performance of Asphalt Pavements on Coastal Hot and Humid Highways, Grant No. GuikeAB22080091). Their assistance is sincerely appreciated.

Conflict of interest

Authors HY, LH, and HC were employed by Guangxi Xinfazhan Communication Group Co.,LTD., Author ZY was employed by Guangxi Transportation Science and Technology Co.,LTD.

The remaining authors declare that the research was conducted in the absence of any commercial or financial relationships that could be construed as a potential conflict of interest.

Generative AI statement

The author(s) declare that no Generative AI was used in the creation of this manuscript.

Publisher's note

References

Abdelsalam, M., Yue, Y. C., Khater, A., Luo, D., Musanyufu, J., and Qin, X. (2020). Laboratory study on the performance of asphalt mixes modified with a novel composite of diatomite powder and lignin fiber. *Appl. Sciences-Basel* 10 (16), 5517. doi:10.3390/app10165517

Abu, Q., Nazzal, M. D., Abbas, A., Kaya, S., Akinbowale, S., Arefin, M. S., et al. (2018). Micromechanical and chemical characterization of foamed warm-mix asphalt aging. *J. Mater. Civ. Eng.* 30. doi:10.1061/(ASCE)MT.1943-5533.0002430

Almeida, A., and Picado, L. (2023). Asphalt road pavements to address climate change challenges-an overview. *Appl. Sciences-Basel* 12 (24), 12515. doi:10.3390/app122412515

Alnadish, A. M., Aman, M. Y., Katman, H. Y. B., and Ibrahim, M. R. (2021). Characteristics of warm mix asphalt incorporating coarse steel slag aggregates. *Appl. Sciences-Basel* 11 (8), 3708. doi:10.3390/app11083708

American Association of State Highway and Transportation Officials (AASHTO) (2003). *Standard method of test for determining the fatigue life of compacted hot-mix asphalt (HMA) subjected to repeated flexural bending*. Washington, DC: AASHTO.

Arega, Z. A., Bhasin, A., Li, W., Newcomb, D. E., and Arambula, E. (2013). Characteristics of asphalt binders foamed in the laboratory to produce warm mix asphalt. *J. Mater. Civ. Eng.* 26 (11), 04014078. doi:10.1061/(ASCE)MT.1943-5533.0000981

Bairgi, B. K., Mannan, U. A., and Tarefder, R. A. (2019). Tribological approach to demonstrate workability of foamed warm-mix asphalt. *J. Mater. Civ. Eng.* 31 (9), 04019191. doi:10.1061/(ASCE)MT.1943-5533.0002843

Bairgi, B. K., Tarefder, R. A., and Ahmed, M. U. (2018). Long-term rutting and stripping characteristics of foamed warm-mix asphalt (WMA) through laboratory and field investigation. *Constr. Build. Mater.* 170 (10), 790–800. doi:10.1016/j.conbuildmat.2018.03.055

Fan, Y. H., Sun, L. J., Zhang, C. Q., Xu, J., Liu, J., and Wang, C. (2024). Molecular dynamics-based study of graphene/asphalt mechanism of interaction. *Appl. Sciences-Basel* 14 (14), 6168. doi:10.3390/app14146168

Ghabchi, R., Singh, D., Zaman, M., and Hossain, Z. (2016). Laboratory characterisation of asphalt mixes containing RAP and RAS. *Int. J. Pavement Eng.* 17 (9), 829–846. doi:10.1080/10298436.2015.1022778

Guo, W., Guo, X. D., Li, Y. S., and Dai, W. (2020). Laboratory investigation on physical, rheological thermal and microscopic characteristics of water-foamed asphalt under three environmental conditions. *Coatings* 10 (3), 239. doi:10.3390/coatings10030239

Hande, I., and Ozturk, M. (2018). Sensitivity of nozzle-based foamed asphalt binder characteristics to foaming parameters. *Transp. Res. Rec.* 2444 (1), 120–129. doi:10.3141/2444-14

Hu, J. Y., Ma, T., Yin, T., and Zhou, Y. (2022). Foamed warm mix asphalt mixture containing crumb rubber: foaming optimization and performance evaluation. *J. Clean. Prod.* 333, 130085. doi:10.1016/j.jclepro.2021.130085

Huang, A., Liu, G., Mouillet, V., Somé, S. C., Cao, T., and Huang, H. (2022). Rheological and chemical evolution of hma and wma binders based on ageing kinetics. *Materials* 15 (2), 679. doi:10.3390/ma15020679

Iwanski, M., Chomicz, K. A., Maciejewski, K., Janus, K., Radziszewski, P., Liphardt, A., et al. (2023). Stiffness Evaluation of laboratory and plant produced foamed bitumen warm asphalt mixtures with fiber reinforcement and bio-flux additive. *Materials* 16 (5), 1950. doi:10.3390/ma16051950

Khosravifar, S., Haider, I., Afsharikia, Z., and Schwartz, C. W. (2015). Application of time–temperature superposition to develop master curves of cumulative plastic strain in repeated load permanent deformation tests. *Int. J. Pavement Eng.* 16 (3), 214–223. doi:10.1080/10298436.2014.937810

Liu, S. J., Zhou, S. B., and Peng, A. H. (2020). Laboratory evaluation of foamed warm mix binders and mixtures containing reclaimed asphalt pavements. *Constr. Build. Mater.* 258, 119773. doi:10.1016/j.conbuildmat.2020.119773

Ministry of Transport of the People's Republic of China (2011). *Test procedures for bitumen and bituminous mixtures in highway engineering (JTG E20-2011)*. Beijing: China Communications Press.

Ozturk, H. I., and Kutay, M. E. (2014). Novel testing procedure for assessment of quality of foamed warm mix asphalt binders. *J. Mater. Civ. Eng.* 26 (8), 04014042. doi:10.1061/(ASCE)MT.1943-5533.0000924

Qin, Y., Huang, S., Xu, J., and Li, F. (2009). Test and analysis of energy saving and emission reduction of warm mixed asphalt. *J. Highw. Transp. Res. Dev.* 26 (8), 33–37. doi:10.1016/j.conbuildmat.2019.03.005

Qin, Y., Huang, S., Xu, J., Li, F., and Sun, L. (2010). Performance of SMA mixture based on Evotherm-DAT warm mix asphalt technology. *J. Build. Mater.* (01), 36–39. doi:10.3969/i.issn.1007-9629.2010.01.007

Song, K., Chen, J., Fan, W., and Shen, J. (2015). Volumetric property of water foamed warm-mix asphalt mixture based on orthogonal experiment. *J. Highw. Transp. Res. Dev.* 32 (10), 19–24. doi:10.3969/i.issn.1002-0268.2015.10.004

Sun, Z. W., Kou, C. J., Lu, Y., Wu, Z., Kang, A., and Xiao, P. (2024). A Study of the bond strength and mechanism between basalt fibers and asphalt binders. *Appl. Sciences-Basel* 14 (6), 2471. doi:10.3390/app14062471

Wang, G. S., and Liu, Z. L. (2017). Viscosity change of warm-mix asphalt in different foaming conditions. *Road Mach. and Constr. Mech.* 34 (007), 46–49. doi:10.14059/i.issn.1871-2599.2017.05.049

Wang, J., Qin, Y., Xu, J., Zeng, W., Zhang, Y., Wang, W., et al. (2020). Crack resistance investigation of mixtures with reclaimed SBS modified asphalt pavement using the SCB and DSCT tests. *Constr. Build. Mater.* 265, 120365. doi:10.1016/j.conbuildmat.2020.120365

Wei, W. J., Zheng, B. F., Han, C., Niu, X., and Yan, J. (2017). Evaluation method of anti-water damage performance of foamed warm-mix asphalt based on surface free energy. *Highway* (02), 200–204. doi:10.3141/2402-05

Wen, Y. K., Gui, N. S., Wang, L., Gu, W., and You, Z. (2020). Analysis of rheological properties and micromechanism of foamed warm mix asphalt mastic. *Mater. Rep.* (10), 10052–10060. doi:10.11896/cldb.19050044

Woszuk, A., and Franus, W. (2017). A review of the application of zeolite materials in warm mix asphalt technologies. *Appl. Sciences-Basel* 7 (3), 293. doi:10.3390/app7030293

Xu, J., Yang, E., Wang, S., and Wang, L. (2020). Study on low temperature performance evaluation indictor of sasobit warm mix asphalt. *J. Highw. Transp. Res. Dev.* 37 (2), 8–14. doi:10.3969/i.issn.1002-0268.2020.02.002

You, Z., Porter, D., Yang, X., and Yin, H. (2017). Preliminary laboratory evaluation of methanol foamed warm mix asphalt binders and mixtures. *J. Mater. Civ. Eng.* 29 (11), 06017017. doi:10.1061/(ASCE)MT.1943-5533.0002085

Yu, J. M., Yu, X. S., Gao, Z. M., Guo, F., Wang, D., and Yu, H. (2018). Fatigue resistance characterization of warm asphalt rubber by multiple approaches. *Appl. Sciences-Basel* 8 (9), 1495. doi:10.3390/app8091495

Zhou, J., Li, J., Liu, G. Q., Yang, T., and Zhao, Y. (2021). Recycling aged asphalt using hard asphalt binder for hot-mixing recycled asphalt mixture. *Appl. Sciences-Basel* 11 (12), 5698. doi:10.3390/app11125698

Zhu, H., Shen, J., Shi, P., and Chen, J. (2014). Research on volume performance of foamed warm-mixed asphalt mixture. *J. Highw. Transp. Res. Dev.* 31 (8), 19–24. doi:10.3969/i.issn.1002-0268.2014.08.004

Zou, X. Y., Li, Y. T., and Bai, N. (2016). Study on variation law of foaming water content in different construction stages of foamed warm asphalt mixture. *J. China and Foreign Highw.* (2), 218–221. doi:10.14048/i.issn.1671-2579.2016.02.049